Geometry, Light Response and Quantum Transport in Topological States

Karyn Le Hur

Centre de Physique Theorique, Ecole Polytechnique and CNRS France

Home Seminars Registration Contacts Search: ?

03/05/2021, Monday, 17:00–18:00 Europe/Lisbon — Online

Karyn Le Hur, Centre de Physique Theorique, École Polytechnique, CNRS
Geometry, Light Response and Quantum Transport in Topological States of Matter

Topological states of matter are characterized by a gap in the bulk of the system referring to an insulator or a superconductor and topological edge modes as well which find various applications in transport and spintronics. The bulk-edge correspondence is associated to a topological number. The table of topological states include the quantum Hall effect and the quantum anomalous Hall effect, topological insulators and topological superconductors in various dimensions and lattice geometries. Here, we discuss classes of states which can be understood from mapping onto a spin-1/2 particle in the reciprocal space of wave-vectors. We develop a geometrical approach on the associated Poincare-Bloch sphere, developing smooth fields, which shows that the topology can be encoded from the poles only. We show applications for the light-matter coupling when coupling to circular polarizations and develop a relation with quantum transport and the quantum Hall conductivity. The formalism allows to include interaction effects. We show our recent developments on a stochastic approach to englobe these interaction effects and discuss applications for the Mott transition of the Haldane and Kane-Mele models. Then, we develop a model of coupled spheres and show the possibility of fractional topological numbers as a result of interactions between spheres and entanglement allowing a superposition of two geometries, one encircling a topological charge and one revealing a Bell or EPR pair. Then, we show applications of the fractional topological numbers $C = 1/2$ in bilayer honeycomb models describing topological semi-metals characterized by a quantized Berry phase at one Dirac point.

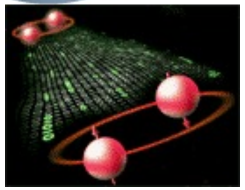

Summary of the presentation

$$\vec{F} = q(\vec{r} \times \vec{B})$$

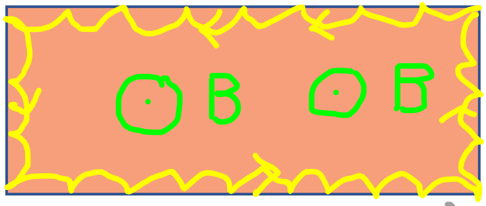

$$\vec{B} = \vec{\nabla} \times \vec{A}$$

Introduction
Quantum Hall state and Fractional Quantum Hall effect

Geometry from the reciprocal space and Poincare-Bloch sphere
Topological properties from the poles and Time
Quantum Transport and Light Response
Interaction Effects
Applications

Fractional topology from the curved space
Application in quantum spheres model and topological semi-metals

Topological Bloch bands

Quantum Hall Effect and Chern Insulator

Haldane model

$$\mathcal{H}_0 = \sum_i (-1)^i M c_i^\dagger c_i - \sum_{<i,j>} t_1 c_i^\dagger c_j - \sum_{\ll i,j \gg} t_2 e^{i\phi_{ij}} c_i^\dagger c_j$$

F. D. M. Haldane, Phys. Rev. Lett. 61, 2015 (1988)

No net flux M = Semenoff mass

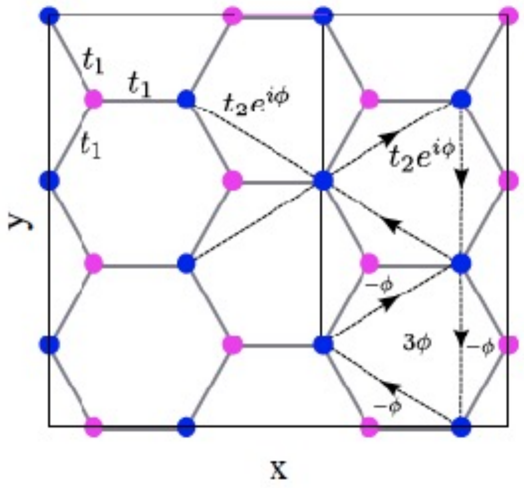

Realized in quantum materials, graphene, cold atoms, light systems

Phase diagrams of interacting
Bosonic & Fermionic Models

I. Vasic, A. Petrescu, K. Le Hur, W. Hofstetter, Phys. Rev. B 91, 094502 (2015)

Ph. Klein, A. Grushin, K. Le Hur, PRB 2021 arXiv:2002.01742

Mott transition and New Methods

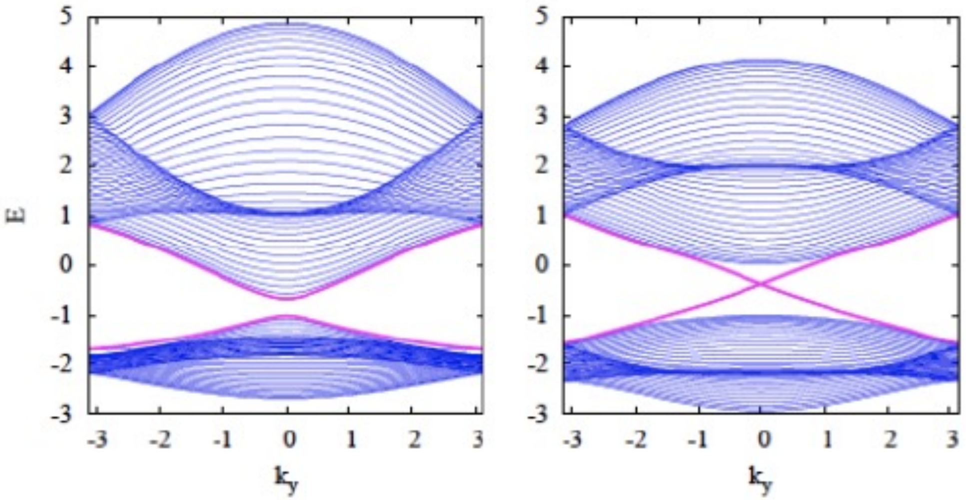

Spin-1/2 analogy

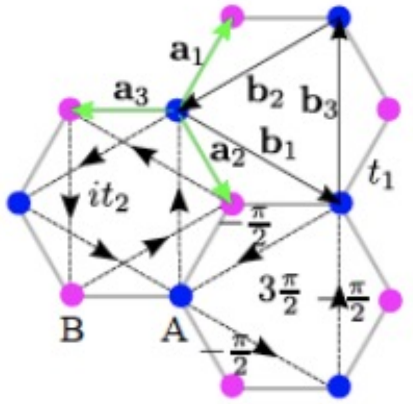

$$\mathcal{H}_{\mathrm{H}}(\mathbf{k}) = -\mathbf{d}\left(\mathbf{k}\right) \cdot \hat{\sigma},$$

We have introduced the field $\psi(\mathbf{k}) = (b_A(\mathbf{k}), b_B(\mathbf{k}))^T$ of Fourier transforms of the annihilation operators for bosons on sublattices A and B. We wrote $\mathcal{H}_{\mathrm{H}}$ in the basis of Pauli matrices $\hat{\sigma} = (\sigma_x, \sigma_y, \sigma_z)$ in terms of

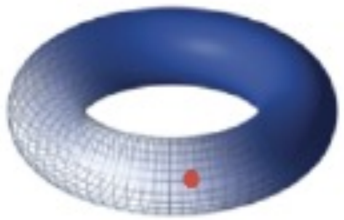

$$\mathbf{d}(\mathbf{k}) = \left(t_1 \sum_i \cos \mathbf{k}\, \mathbf{a_i}, t_1 \sum_i \sin \mathbf{k}\, \mathbf{a_i}, -2t_2 \sum_i \sin \mathbf{k}\, \mathbf{b_i}\right).$$

The non-trivial topology of the Bloch bands translates to a nonzero winding number of the map $\hat{\mathbf{d}} = \mathbf{d}/|\mathbf{d}|$ from the torus (the first Brillouin zone) to the unit sphere.

$\{ K \leftrightarrow$ north
$K' \leftrightarrow$ south

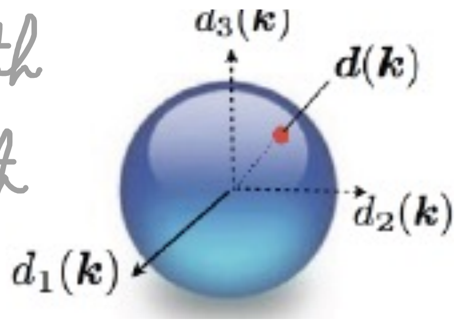

$$\boxed{\mathcal{C}_- = \frac{1}{4\pi} \int_{\mathrm{BZ}} d\mathbf{k}\, \hat{\mathbf{d}} \cdot \left(\partial_1 \hat{\mathbf{d}} \times \partial_2 \hat{\mathbf{d}}\right)}$$

$\mathbb{Z}$

$\mathcal{C} = (0, \pm 1)$

spin - $\frac{1}{2}$

Topology

Euler characteristic is defined as

$$\chi = V - E + F$$

where V is the number of vertices (corners), E edges and F faces.

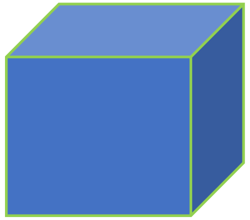

Take a cube. What is the Euler characteristic? Is this non-zero? $\chi = 2$

Sphere	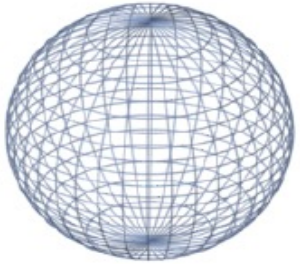	2

OR Euler characteristic for an orientable surface:

$$\chi = 2 - 2g$$

where g can be seen simply as the number of holes. For a sphere, one may say that in that case $g = 0$ and $\chi = 2$. We want to make a link between g and topological properties of the lattice.

Question: Can we change a sphere in a coffee cup?

Topological Properties on the sphere

From the analogy of the Bohr's quantization for the angular momentum or wave-vector in a closed orbit trajectory, one may introduce an observable on the sphere traducing the behavior of the wave-vector (M. Berry, 1984)

$$\boxed{\mathbf{A} = i\langle\psi|\nabla|\psi\rangle}$$

$\vec{P} \mapsto i\hbar\vec{\nabla}$

From the analogy with Gauss' law, we want to show that a radial magnetic field acting on the surface of the sphere S^2 produces a topological charge at the center of the sphere. A radial magnetic field on the sphere has the same properties as the Haldane model in **k**-space. The model on the sphere is then $H = -\mathbf{d} \cdot \hat{\mathbf{S}}$ with $\hat{\mathbf{S}} = \hbar/2\hat{\sigma}$

$$\vec{d} = d_0(\sin\theta\cos\varphi, \sin\theta\sin\varphi, \cos\theta).$$

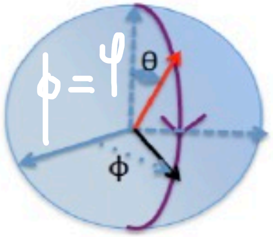

Remind briefly the matrix form:

$$\vec{S} = \frac{\hbar}{2}\begin{pmatrix} \cos\theta & e^{-i\varphi}\sin\theta \\ e^{i\varphi}\sin\theta & -\cos\theta \end{pmatrix}$$

The ground state corresponds to the state

$$\boxed{|+\rangle_{\vec{r}} = e^{-i\varphi/2}\cos\frac{\theta}{2}|+\rangle_z + e^{i\varphi/2}\sin\frac{\theta}{2}|-\rangle_z.}$$

$C = +1$

The surface $S^{2'}$ can be decomposed as a north (north') hemisphere and south (south') hemispheres and the fields $\mathbf{A}$ are smooth on $S^{2'}$, such that

$$C = -\frac{1}{2\pi}\int_{north'} \nabla \times \mathbf{A}_N d^2\mathbf{n} - \frac{1}{2\pi}\int_{south'} \nabla \times \mathbf{A}_S d^2\mathbf{n}.$$

On north', we have from Stokes' theorem:

$$-\frac{1}{2\pi}\int_{north'} \nabla \times \mathbf{A}_N d^2\mathbf{n} = -\frac{1}{2\pi}\int_0^{2\pi} d\varphi A_{N\varphi}(\varphi, \theta_c) + \frac{1}{2\pi}\int_0^{2\pi} d\varphi A_\varphi(0).$$

This form assumes that the field is uniquely defined on the boundary path at the north pole with $A_\varphi(0) = A_{N\varphi}(\varphi, 0)$. The right-hand side then corresponds to the two boundary paths encircling $north'$. Similarly, we have for $south'$

$$-\frac{1}{2\pi}\int_{south'} \nabla \times \mathbf{A}_S d^2\mathbf{n} = +\frac{1}{2\pi}\int_0^{2\pi} d\varphi A_{S\varphi}(\varphi, \theta_c) - \frac{1}{2\pi}\int_0^{2\pi} d\varphi A_\varphi(\pi).$$

The field is uniquely defined on the boundary path at the south pole with $A_\varphi(\pi) = A_{S\varphi}(\varphi, \pi)$. We can then define the smooth fields as

$$A'_{N\varphi}(\varphi, \theta) = A_{N\varphi}(\varphi, \theta_c) - A_\varphi(0)$$

$$A'_{S\varphi}(\varphi, \theta) = A_{S\varphi}(\varphi, \theta_c) - A_\varphi(\pi)$$

Chern number

$$\boxed{C = -\frac{1}{2\pi}\int_{S^{2'}} \nabla \times \mathbf{A} d^2\mathbf{n}.}$$

$\vec{F} = \vec{\nabla} \times \vec{A}$

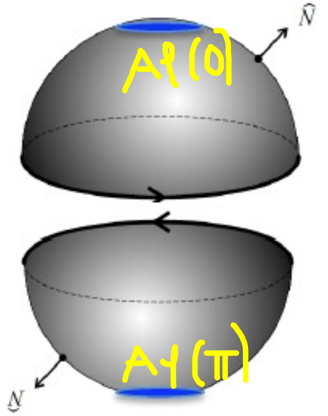

smooth fields, poles:

$A'_{N\varphi} \to 0$, $A_{S\varphi} \to 0$

$$\boxed{\oint \mathbf{A}' \cdot d\mathbf{l} = \oint \mathbf{A} \cdot d\mathbf{l} - \oint_{r=r_c} \mathbf{A}_\varphi(pole) \cdot d\mathbf{l}.}$$

$$\boxed{C = -\frac{1}{2\pi}\int_0^{2\pi} d\varphi A'_{N\varphi}(\varphi,\theta_c) + \frac{1}{2\pi}\int_0^{2\pi} d\varphi A'_{S\varphi}(\varphi,\theta_c)}$$

Joel Hutchinson
Karyn Le Hur

arXiv: 2002.11823

$$A'_{N\varphi} = \sin^2\frac{\theta}{2}$$

$$A'_{S\varphi} = -\cos^2\frac{\theta}{2}$$

(almost) accepted by Communication Physics, Nature Journal Today

Therefore, we obtain that for any boundary with θ_c:

$$-\frac{1}{2\pi}\int_0^{2\pi} d\varphi (A'_{N\varphi} - A'_{S\varphi}) = C$$

allows fractional numbers

We can therefore move the 2 circles close to the small disks at north and south poles and reveal the additivity of Berry phases. Producing edge states in k-space is also interesting to probe the light-matter coupling response where light is circularly polarized. The physics is analogous to the nuclear magnetic resonance.

Equivalent formulation in terms of the poles

$$-\frac{1}{2\pi}\int_{north'} \nabla\times\mathbf{A}_N d^2\mathbf{n} = -\frac{1}{2\pi}\int_0^{2\pi} d\varphi A_{N\varphi}(\varphi,\theta_c) + \frac{1}{2\pi}\int_0^{2\pi} d\varphi A_\varphi(0) \mapsto 0$$

$$-\frac{1}{2\pi}\int_{south'} \nabla\times\mathbf{A}_S d^2\mathbf{n} = +\frac{1}{2\pi}\int_0^{2\pi} d\varphi A_{S\varphi}(\varphi,\theta_c) - \frac{1}{2\pi}\int_0^{2\pi} d\varphi A_\varphi(\pi).$$

$\theta_c \to 0$ unicity of $A_\varphi(0)$

$A_{N\varphi} = A_\varphi(0)$
$A_{S\varphi} = A_\varphi(0)$

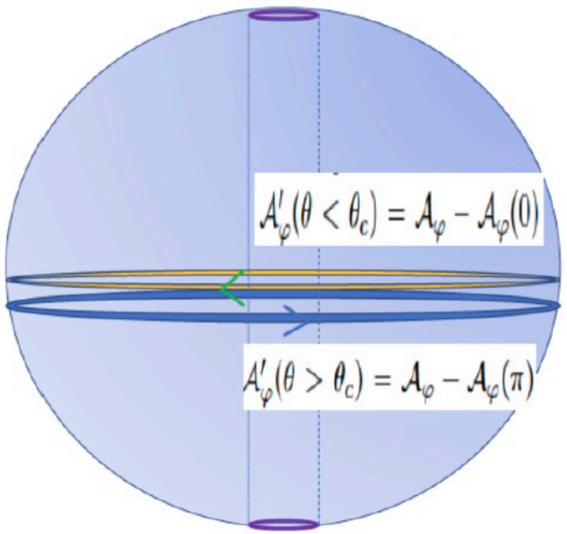

Topological charge

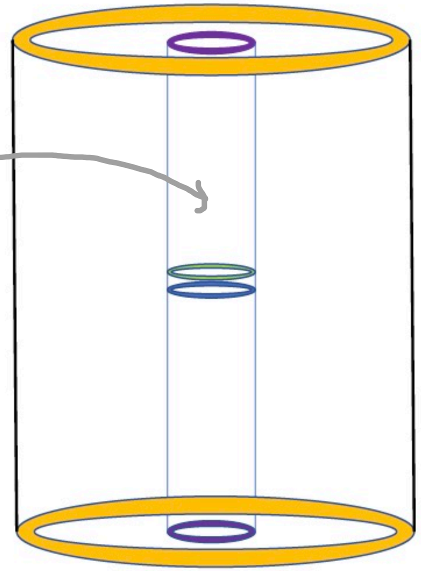

$$\boxed{C = A_\varphi(0) - A_\varphi(\pi)}$$

$$\boxed{C = \frac{1}{2}\left(\langle\sigma_z(0)\rangle - \langle\sigma_z(\pi)\rangle\right)}$$

D. Schroer et al. PRL 2014 (Boulder, K. Lehnert)
P. Roushan et al. Nature (John Martinis, Santa Barbara) 2014
Theory: A. Polkovnikov, V. Gritsev, M. Kolodrubetz

L. Henriet, A. Sclocchi, P. P. Orth, K. Le Hur PRB 2017

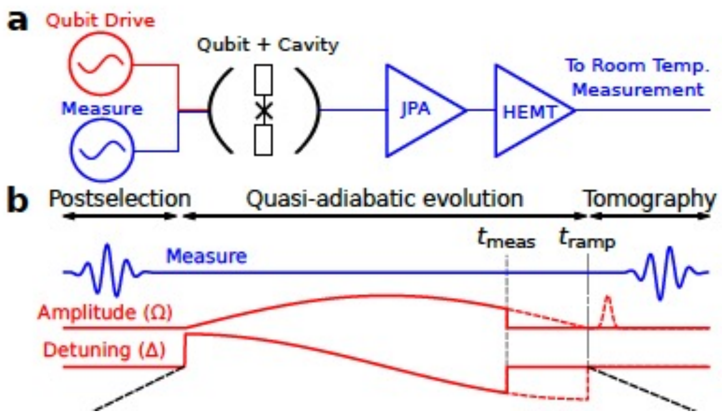

$$H/\hbar = \frac{1}{2}\left[\Delta\, \sigma_z + \Omega\, \sigma_x \cos\phi + \Omega\, \sigma_y \sin\phi\right] \ ,$$

$$\Delta = \Delta_1 \cos\theta + \Delta_2 \ , \ \Omega = \Omega_1 \sin\theta$$

$$\theta(t) = \pi t / t_{\text{ramp}}$$

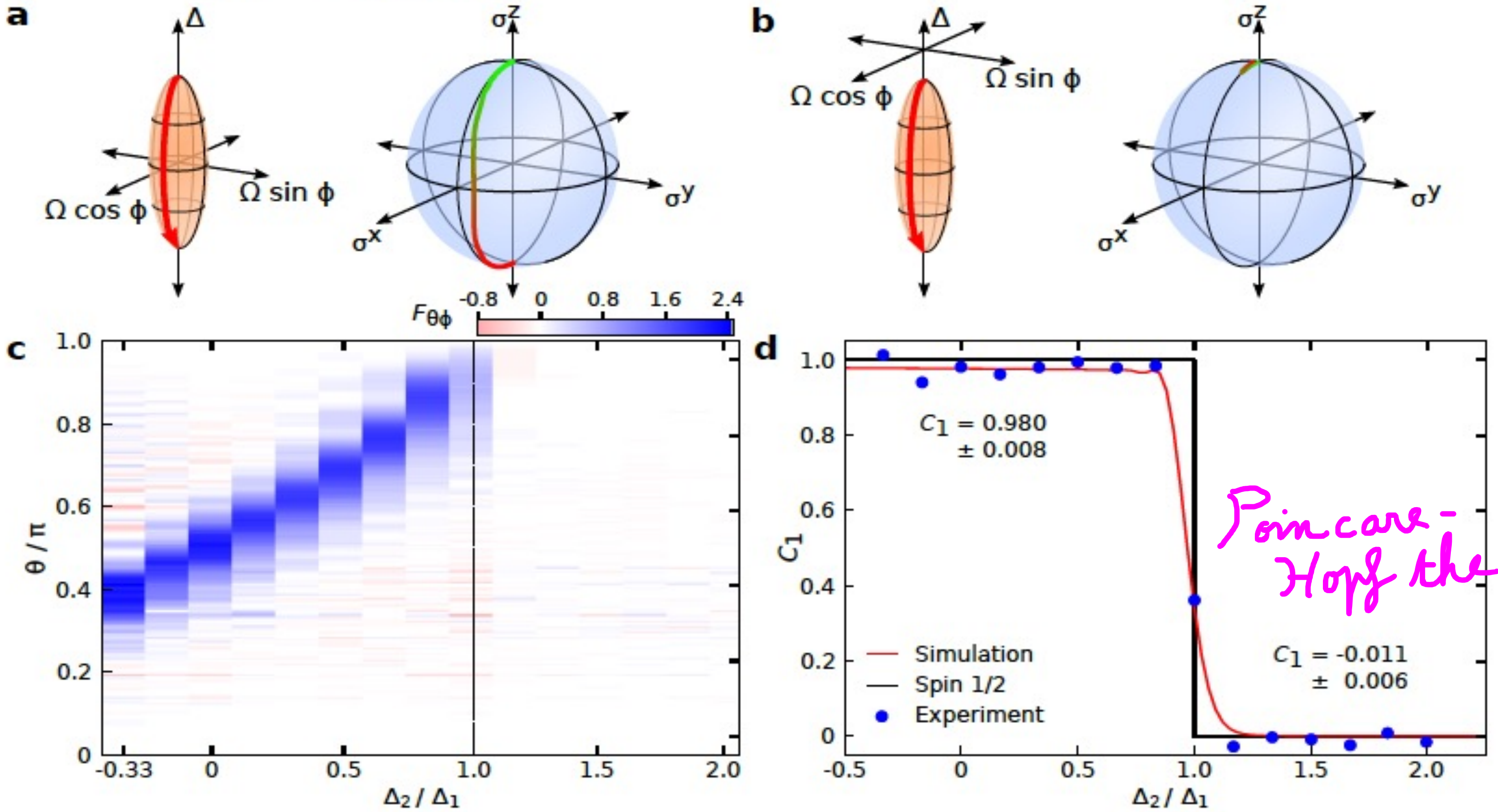

Poincaré-Hopf theorem

Smooth Fields on the Sphere and Topological Observables

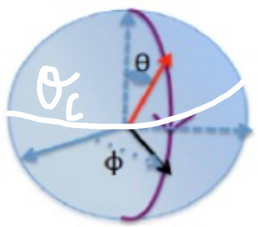

$$\mathbf{E} = E\mathbf{e}_{x_\parallel}$$

$$\hbar k_\parallel = m v_\parallel$$

$$m a_\parallel = \hbar \dot{k}_\parallel = \hbar \partial k_\parallel / \partial t = eE$$

$k_\parallel = \theta;\ k_\perp = \varphi$

$\vec{F} = e\vec{E}$

$\theta = \frac{eE}{\hbar} t$

$$\boxed{J_\perp^e = \frac{e}{T}\int_0^T dt \frac{d\langle x_\perp\rangle}{dt} = \frac{e}{T}\left(\langle x_\perp\rangle(T) - \langle x_\perp\rangle(0)\right) = \frac{e}{T}\oint \frac{d\phi}{2\pi}\left(\psi^*(T,\phi) i \frac{\partial\psi}{\partial\phi} - \psi^*(0,\phi) i \frac{\partial\psi}{\partial\phi}\right)}$$

Then, we define for a fixed angle ϕ

$$J_\phi(\theta,\phi) = \frac{ie}{4\pi T}\left(\psi^* \frac{\partial}{\partial\phi}\psi - \frac{\partial\psi^*}{\partial\phi}\psi\right) = \frac{ie}{2\pi T}\psi^* \frac{\partial}{\partial\phi}\psi$$

such that

$$J_\perp^e(\theta) = \oint d\phi \left(J_\phi(\theta,\phi) - J_\phi(0,\phi)\right).$$

Therefore, we observe a relation between the transverse current density and the smooth fields:

$$J_\perp^e(\theta) = \frac{e}{2\pi T}\oint d\phi \mathcal{A}'_{\phi,\theta<\theta_c}(\theta,\phi).$$

Relation applicable for many-body systems

$$\Delta P = \int_0^T dt j$$

$$j = nev = e\int_{BZ}\frac{dq}{2\pi}v(q),$$

$$\mathbf{v} = (e/\hbar)\mathbf{E}\times\mathbf{F} \text{ with } |\mathbf{v}| = (e/\hbar)E|F_{\phi\theta}|$$

Karplus-Luttinger (1954)

$$\Delta P = -e\int_0^T dt\int_{BZ}\frac{dq}{2\pi}\Omega_{qt}$$

$$F_{\mu\nu} = \partial_\mu A_\nu - \partial_\nu A_\mu$$

$\mu = q = \phi$

$\nu = t = \theta$

Here:

$$\Delta P = e\oint\frac{d\phi}{2\pi}\mathcal{A}'_{\phi,\theta<\theta_c}(\theta,\phi)$$

1D pump

$$|\Delta P| = J_\perp T = eC$$

$$j_{xy} = \frac{e}{2\pi}v^*\left(\mathcal{A}_\phi(0) - \mathcal{A}_\phi(\pi)\right) = \frac{(eC)}{2\pi}v^* = \frac{e^2}{h}CE$$

$$\sigma_{xy} = \frac{e^2}{h}C$$

$$\oint d\phi\frac{T^*}{e}\left(J_\phi(0,\phi) - J_\phi(\pi,\phi)\right) = C$$

Light-Matter Coupling

Circular
Dichroism
Jones Polarizations

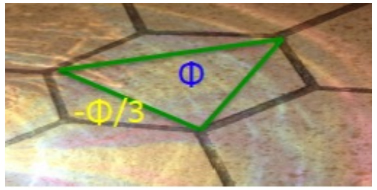

Realization in Hamburg:
Luca Asteria et al. Nature Physics 2019

$$\mathbf{A} = A_0 e^{-i\omega t}(\mathbf{e}_x \mp i\mathbf{e}_y)$$

$$\delta\mathcal{H}_\pm = A_0 e^{\pm i\omega t}|a\rangle\langle b| + h.c.$$

$$\mathcal{H}_+(\omega) = \mathcal{H}_-(-\omega)$$

$$\Gamma_+(\boldsymbol{k}) = \frac{2\pi}{\hbar}|\langle u|\delta\mathcal{H}_\pm|l\rangle|^2\delta(\epsilon_u^{\boldsymbol{k}} - \epsilon_l^{\boldsymbol{k}} - \hbar\omega).$$

[Fermi golden's rule]

$$\int_0^{+\infty} d\omega \frac{1}{2\pi}\oint dl \sum_{\mathbf{k}=\mathbf{K},\mathbf{K}'} \frac{(\boldsymbol{\Gamma}_+(\mathbf{k},\omega) - \boldsymbol{\Gamma}_-(-\mathbf{k},\omega))}{2} = \frac{2\pi}{\hbar^2}A_0^2 C.$$

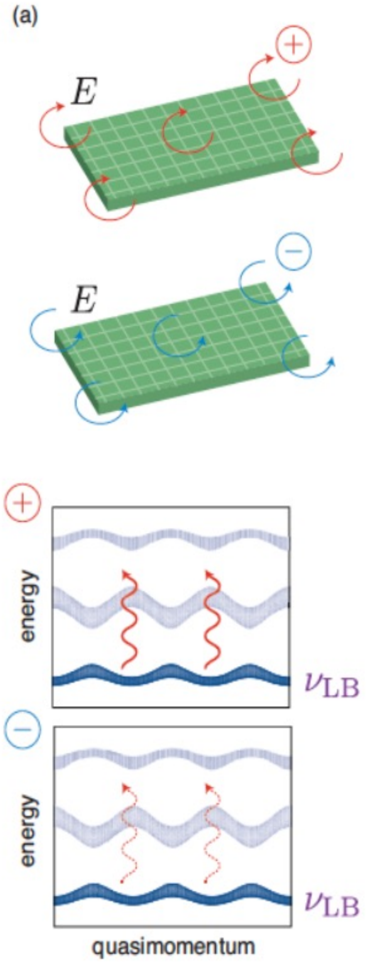

D. Tran, A. Dauphin, A. G. Grushin, P. Zoller, N. Goldman Sciences Advances 2017

Relation to Transport

$$j(t) = \frac{d}{dt}(\hat{n}_a(\mathbf{k}) - \hat{n}_b(\mathbf{k})) = \frac{d}{dt}\sigma^z(\mathbf{k}).$$

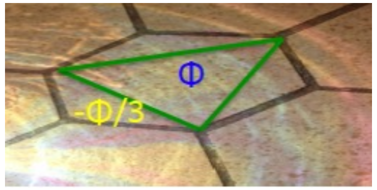

From Ehrenfest Theorem

$$\frac{d}{dt}\sigma^z(\mathbf{k}) = \frac{2}{\hbar}\left((p_x + A_x)\frac{\partial \mathcal{H}}{\partial p_y} - (p_y + A_y)\frac{\partial \mathcal{H}}{\partial p_x}\right).$$

$$\bar{j}(\mathbf{k}) = \frac{2}{\hbar}\left(A_x\frac{\partial \mathcal{H}}{\partial p_y} - A_y\frac{\partial \mathcal{H}}{\partial p_x}\right).$$

$$\boxed{\Gamma_\pm = \frac{2\pi}{\hbar}\sum_{\mathbf{k}=\mathbf{K},\mathbf{K}'}\frac{A_0^2}{\hbar^2}\left|\left\langle u\left|\left(\frac{\partial \mathcal{H}}{\partial p_y} \pm i\frac{\partial \mathcal{H}}{\partial p_x}\right)\right|l\right\rangle\right|^2 \delta(\epsilon_u^{\mathbf{k}} - \epsilon_l^{\mathbf{k}} - \hbar\omega).}$$

Link with Quantum Hall conductivity
Thouless, Kohmoto, Nightingale, deNijs

Within our approach, the sum is performed only on the Dirac points.

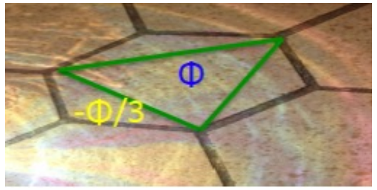

Stochastic View of Interactions

Haldane model $+ V n_A n_B$

$$\mathcal{Z} = \int \mathrm{D}(\Psi, \Psi^\dagger, \phi^0, \phi^x, \phi^y, \phi^z) e^{-\mathcal{S}},$$

$$\mathcal{S} = \int_0^\beta \mathrm{d}\tau \sum_{\boldsymbol{k}} \Psi_{\boldsymbol{k}}^\dagger \left(\partial_\tau + \boldsymbol{h}_0(\boldsymbol{k}) \cdot \boldsymbol{\sigma}\right) \Psi_{\boldsymbol{k}} + \sum_{\boldsymbol{k},\boldsymbol{q},\boldsymbol{p}} \Psi_{\boldsymbol{q}}^\dagger h_V(\boldsymbol{k},\boldsymbol{q},\boldsymbol{p}) \Psi_{\boldsymbol{k}} + \sum_{\boldsymbol{k},r} 6V \phi_{\boldsymbol{k}}^r \phi_{-\boldsymbol{k}}^r,$$

$$\mathcal{H}_{\mathrm{mf}}(\boldsymbol{k}) = \begin{pmatrix} \gamma(\boldsymbol{k}) - 3V(\phi^0 + \frac{1}{2}) & -g(\boldsymbol{k}) \\ -g^*(\boldsymbol{k}) & -\gamma(\boldsymbol{k}) - 3V(\phi^0 + \frac{1}{2}) \end{pmatrix},$$

$$\gamma(\boldsymbol{k}) = 3V\phi^z - 2t_2 \sum_p \sin(\boldsymbol{k} \cdot \boldsymbol{b}_p),$$

$$g(\boldsymbol{k}) = [t_1 - V(\phi^x + i\phi^y)] \sum_p \left(\cos(\boldsymbol{k} \cdot \boldsymbol{a}_p) - i \sin(\boldsymbol{k} \cdot \boldsymbol{a}_p)\right).$$

Stochastic

DMRG

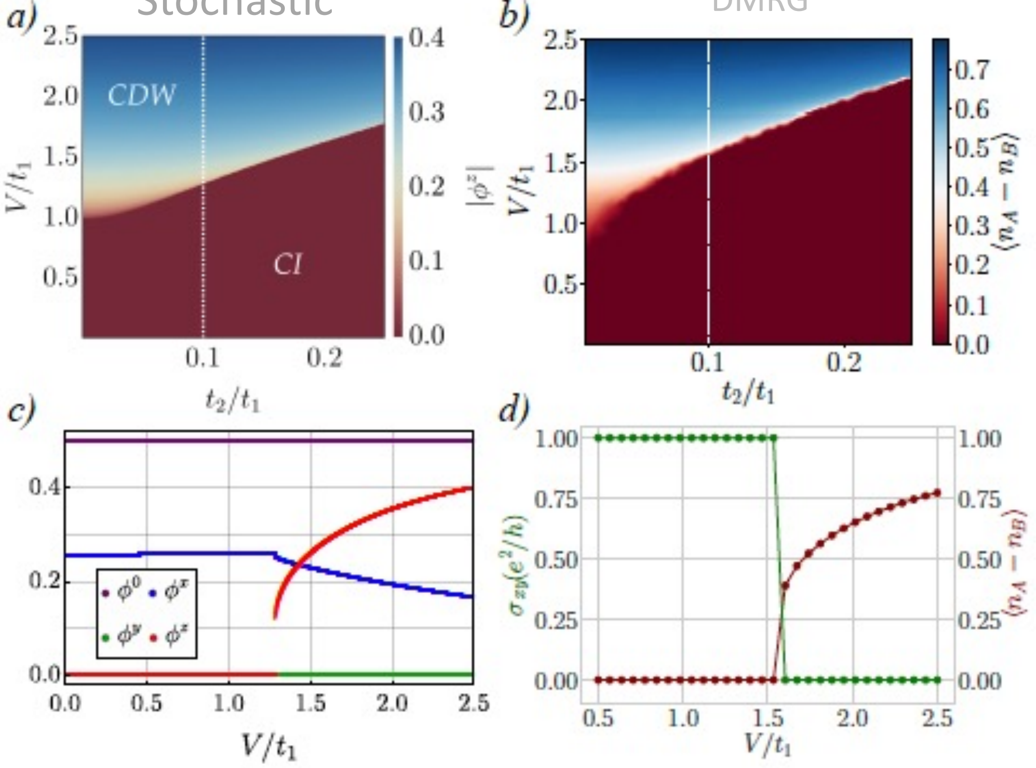

Coupling with Light

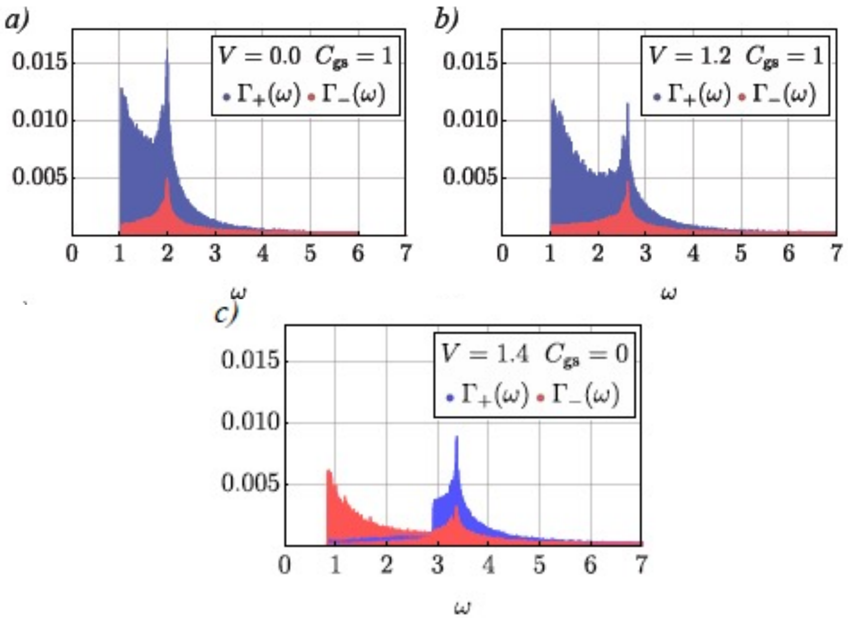

Philipp Klein, Adolfo Grushin, Karyn Le Hur, Phys. Rev. B 2021

Driving in cold atoms

Munich's group

T. Li et al. Science 2016, arXiv:1509.02185

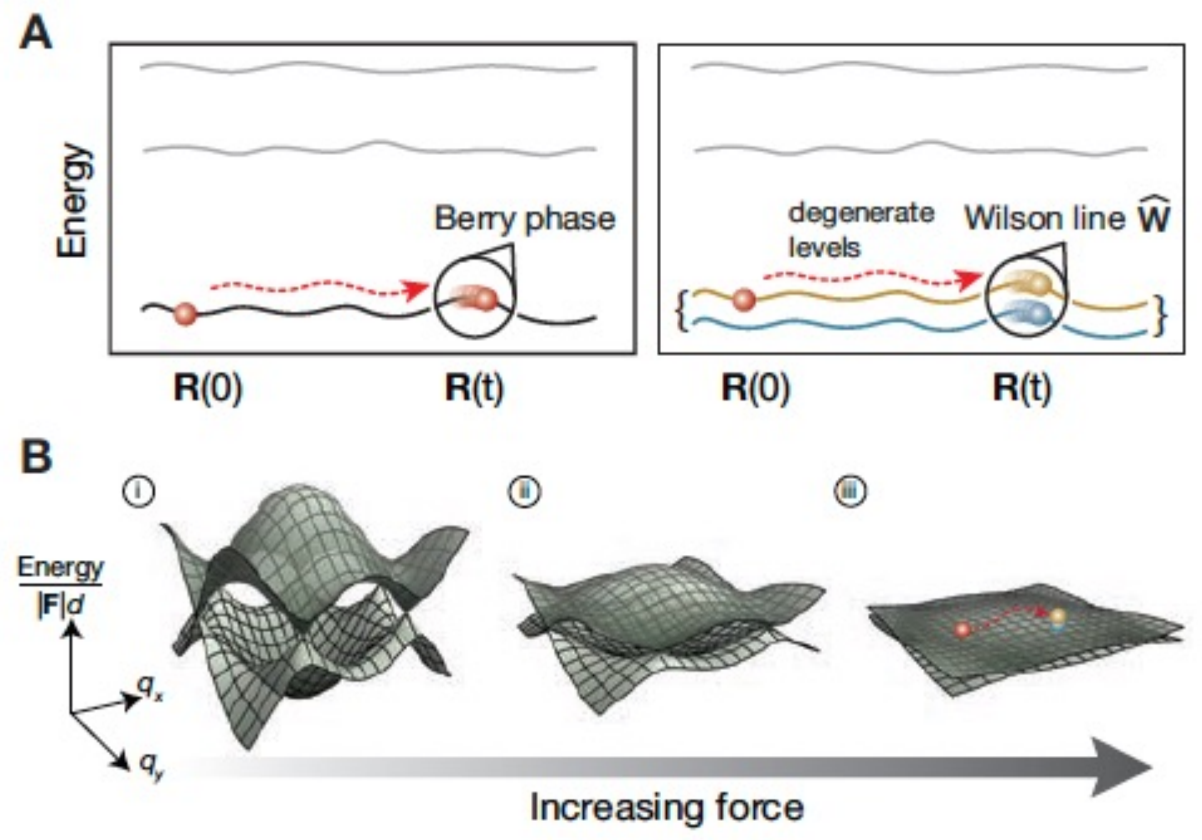

$$\mathbf{q}(t) = \mathbf{q}(0) + \mathbf{F}t/\hbar$$

$$W^{mn}_{\mathbf{Q}\to\mathbf{q}} = \langle \Phi^m_{\mathbf{q}} | e^{i(\mathbf{q}-\mathbf{Q})\cdot\hat{\mathbf{r}}} | \Phi^n_{\mathbf{Q}} \rangle = \langle u^m_{\mathbf{q}} | u^n_{\mathbf{Q}} \rangle.$$

$$|u^1_{\mathbf{q}}\rangle = \cos\frac{\theta_{\mathbf{q}}}{2}|1\rangle + \sin\frac{\theta_{\mathbf{q}}}{2} e^{i\phi_{\mathbf{q}}}|2\rangle.$$

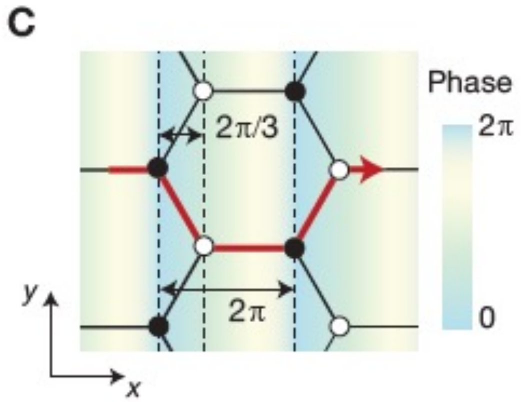

θ_q

$\downarrow$

A'_φ

In principle, current measurable

Topological Insulators & Quantum Spin Hall Effect

- Time-reversal invariant band insulator
- Strong spin-orbit interaction $\lambda \vec{L} \cdot \vec{\sigma}$
- Gapless helical edge mode (Kramers pair)

Mercury, Wurzburg
Bismuth, Princeton

$\mathbb{Z}_2$

$C_\uparrow - C_\downarrow = 2$

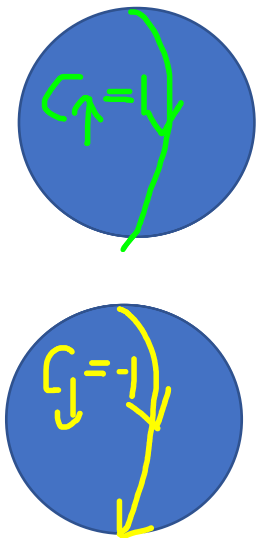

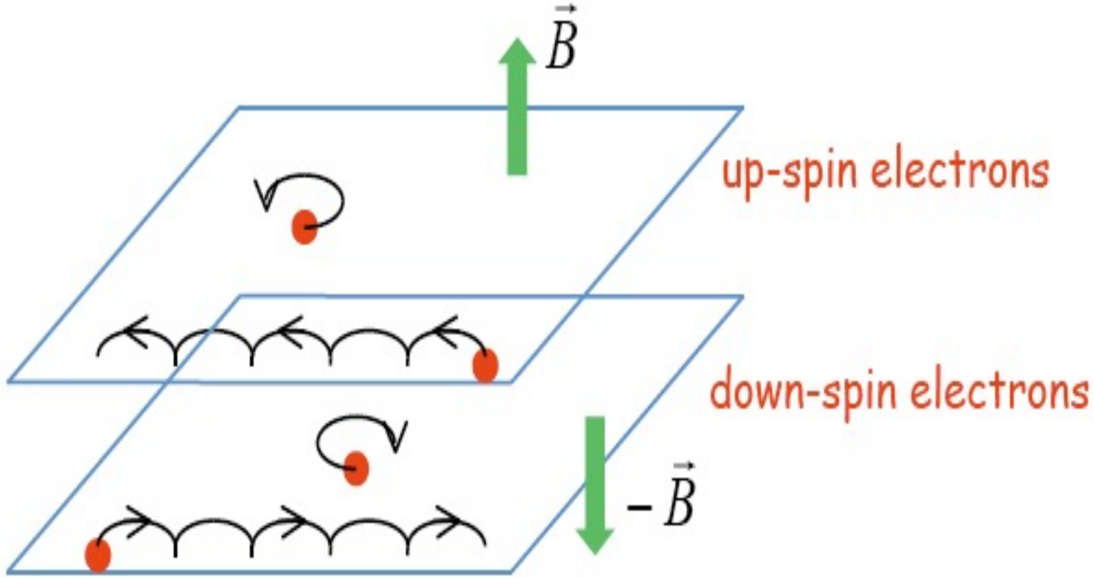

Kane-Mele Model 2005, 2006; L. Fu

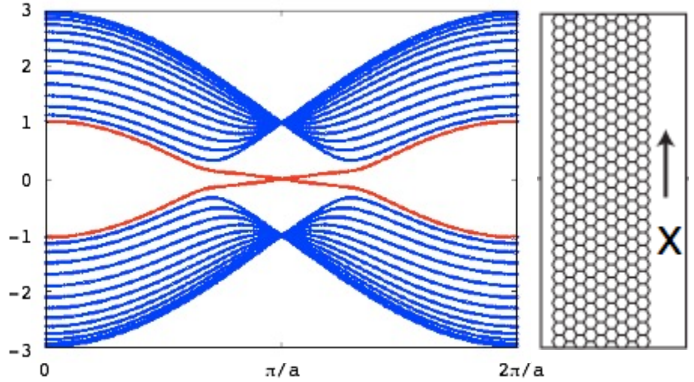

S. C. Zhang, A. Bernevig
helical edge states

Interaction Effects + Mott Physics : S. Rachel and K. Le Hur (2010); W. Wu et al. (CDMFT, 2012); F. Assaad et al. (2010, QMC)
Analytical Solution of Mott Transition: J. Hutchinson, Ph. Klein, K. Le Hur (2021), to appear

2 spheres model

Fractional Topological Numbers

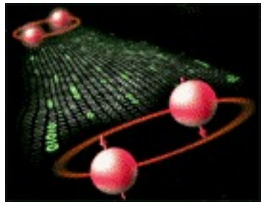

Joel Hutchinson and Karyn Le Hur, arXiv:2002.11823

$$\mathcal{H}^{\pm} = -(\boldsymbol{H}_1 \cdot \boldsymbol{\sigma}^1 \pm \boldsymbol{H}_2 \cdot \boldsymbol{\sigma}^2) \pm \tilde{r} f(\theta) \sigma_z^1 \sigma_z^2$$

$$\boldsymbol{H}_i = (H \sin\theta \cos\phi, H \sin\theta \sin\phi, H \cos\theta + M_i),$$

$$\mathcal{C}^i = -(\mathcal{A}_\phi^i(\pi) - \mathcal{A}_\phi^i(0)).$$

$C^j = \frac{1}{2}$

$$\mathcal{C}^j = \frac{1}{2}\Big(\langle \sigma_z^j(\theta = 0)\rangle - \langle \sigma_z^j(\theta = \pi)\rangle\Big).$$

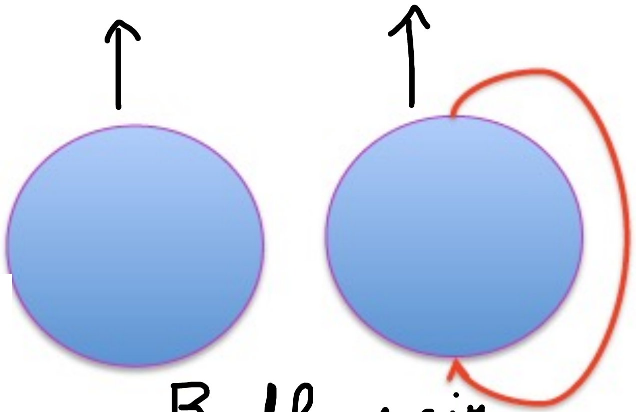

Bell pair

$|\psi\rangle = \frac{1}{\sqrt{2}}(\uparrow\downarrow + \downarrow\uparrow)$

Einstein-Podolsky-Rosen

Model

Joel Hutchinson & Karyn Le Hur
arXiv 2002.11823

Kane-Mele model $\mathcal{H}^-$ with $\tilde{r}=0$

$\vec{H}_1 = -\vec{H}_2$

$$\mathcal{H}^{\pm} = -(\boldsymbol{H}_1 \cdot \boldsymbol{\sigma}^1 \pm \boldsymbol{H}_2 \cdot \boldsymbol{\sigma}^2) \pm \tilde{r} f(\theta) \sigma_z^1 \sigma_z^2 .$$

$\mathcal{H}_+$

$$\boldsymbol{H}_i = (H \sin\theta \cos\phi, H \sin\theta \sin\phi, H\cos\theta + M_i)$$

$f(\theta) = cst$

$\theta = 0$ $|\uparrow\uparrow\rangle$

$$E_{\uparrow\uparrow} = -2H - M_1 - M_2 + \tilde{r} f(0)$$
$$E_{\uparrow\downarrow} = -M_1 + M_2 - \tilde{r} f(0)$$
$$E_{\downarrow\uparrow} = M_1 - M_2 - \tilde{r} f(0)$$
$$E_{\downarrow\downarrow} = 2H + M_1 + M_2 + \tilde{r} f(0),$$

$\theta = \pi$ $\frac{1}{\sqrt{2}}(|\uparrow\downarrow\rangle + |\downarrow\uparrow\rangle)$

$$E_{\uparrow\uparrow} = 2H - M_1 - M_2 + \tilde{r} f(\pi)$$
$$E_{\uparrow\downarrow} = -M_1 + M_2 - \tilde{r} f(\pi)$$
$$E_{\downarrow\uparrow} = M_1 - M_2 - \tilde{r} f(\pi)$$
$$E_{\downarrow\downarrow} = -2H + M_1 + M_2 + \tilde{r} f(\pi).$$

$M_1 = M_2$
$\mathbb{Z}_2$ symmetry

$$H - M < \tilde{r} < H + M,$$

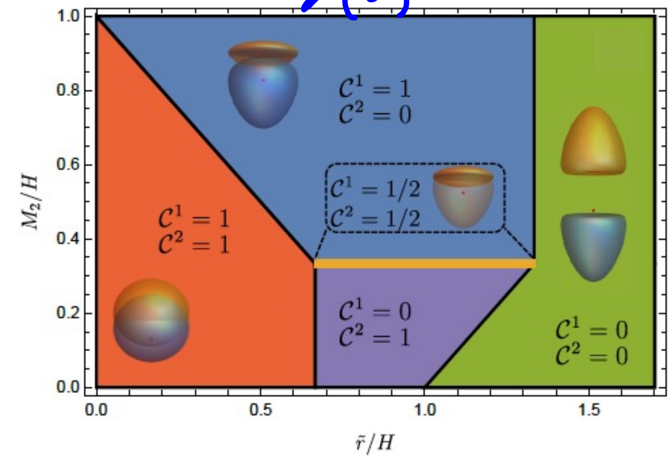

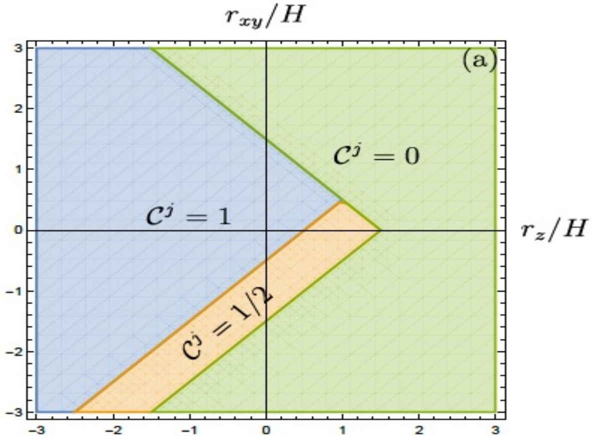

Time-dependent protocol

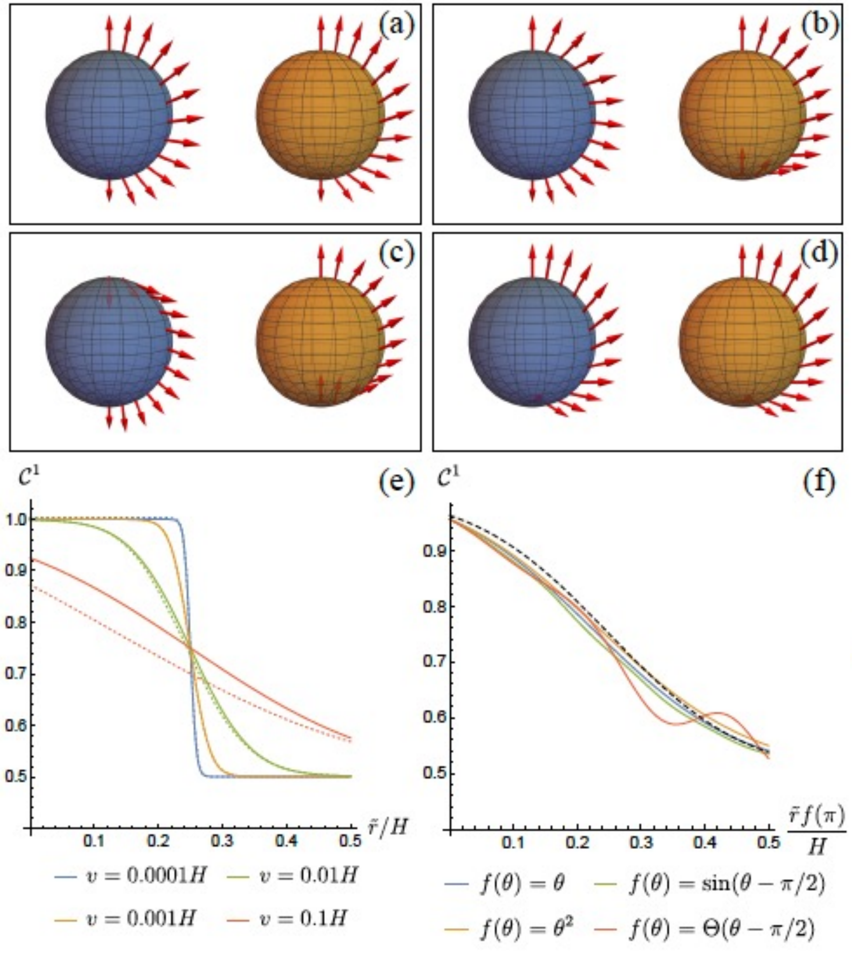

dynamics robust to various forms of interactions

$$\mathcal{C}^j \approx \frac{3}{4} + \frac{\pi}{4}\mathrm{Re}\left(e^{i3\pi/4}e^{-\gamma\pi/4}\frac{\mathrm{sgn}(\Delta)\sqrt{\gamma}}{\Gamma(1/2+i\gamma/4)\Gamma(1-i\gamma/4)}\right),$$

$$\boxed{\mathcal{C}^j \to \frac{3}{4} - \frac{1}{4}\mathrm{sgn}(\Delta),}$$

$$\mathcal{H}^+_{\mathrm{eff}} \to \sqrt{2}Hvt\sigma_z + [\tilde{r}f(\pi) - H + M]\sigma_x.$$

Effective Landau-Zener model

$$t \to t - \pi/v.$$

$$\lambda \equiv \sqrt{2}Hv, \quad \Delta = \tilde{r}f(\pi) - H + M,$$

$$\gamma = \lambda^2/\Delta$$

Santa-Barbara
arXiv 1407.1585
Nature Physics

The Hamiltonian of this system is given by

$$\mathcal{H}_{2Q} = -\frac{\hbar}{2}[H_0\sigma_1^z + \mathbf{H_1}\cdot\boldsymbol{\sigma_1} + \mathbf{H_2}\cdot\boldsymbol{\sigma_2} - g(\sigma_1^x\sigma_2^x + \sigma_1^y\sigma_2^y)], \tag{5}$$

where 1 and 2 refer to qubit 1 (Q1) and qubit 2 (Q2)

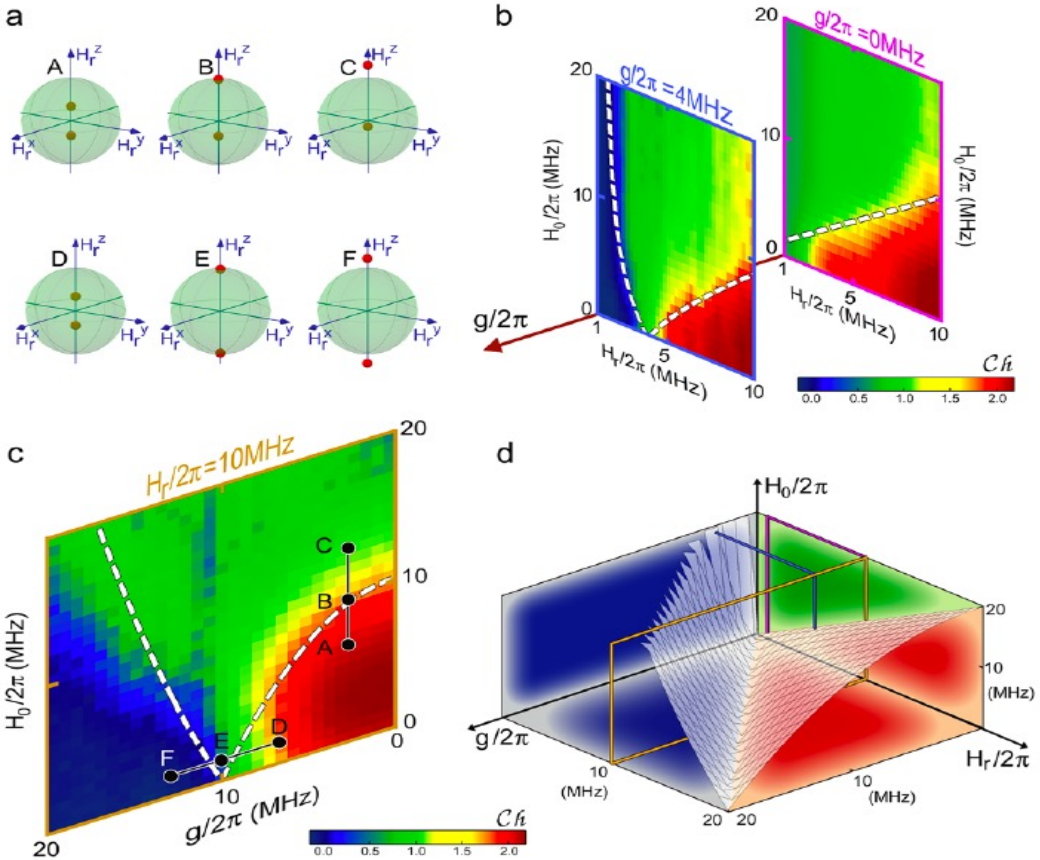

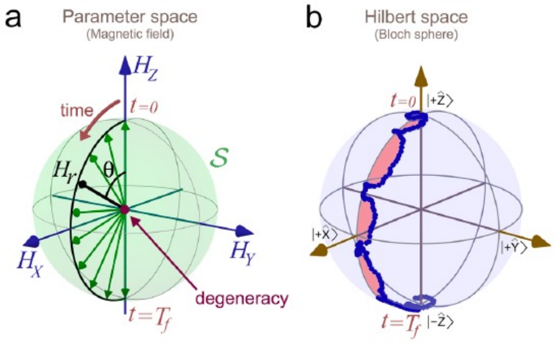

Proximity Effects with Graphene

$C_1 + C_2 = 0$ $\quad C_1 - C_2 = 2$

$\mathbb{Z}_2$ state with asymmetric masses

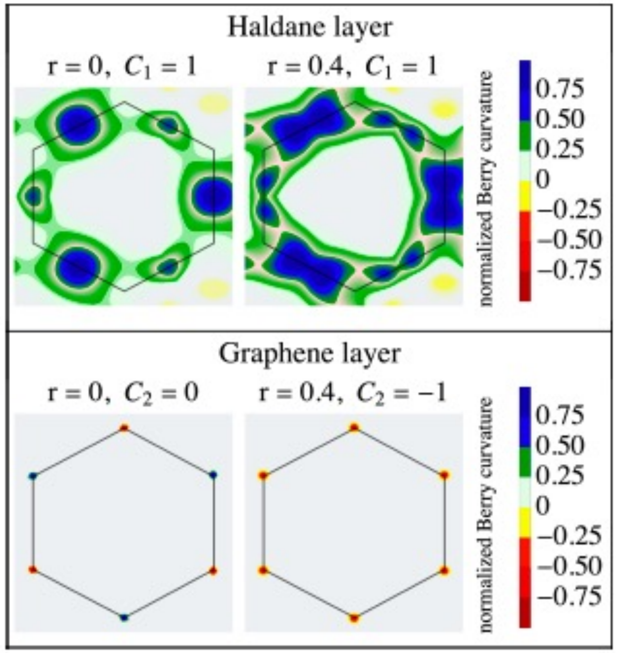

FIG. 1. Berry curvature in the Brillouin zone for the Haldane and graphene layers at $r = 0$ and small r, showing the Berry phase jump effect [35]. Here, $t_1 = 1$ and $t_2 = 1/3$.

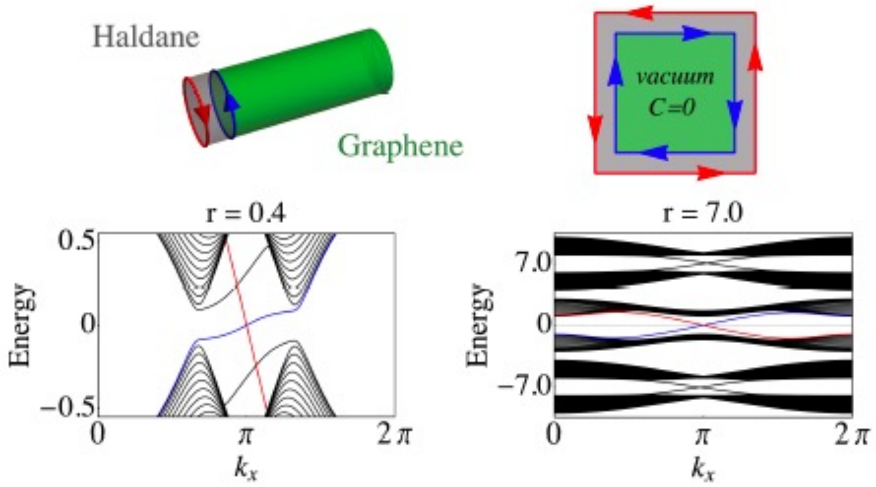

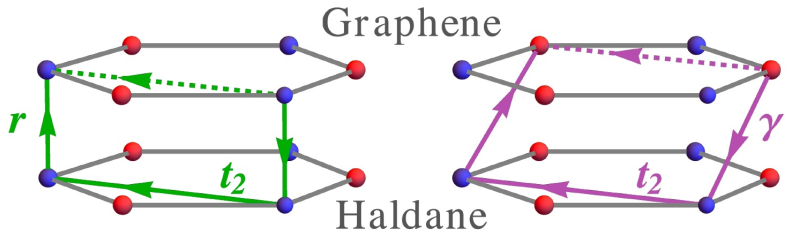

Ising Interaction $\tilde{r}\,\sigma_1^z \sigma_2^z$

interaction in k-space or hopping

Peng Cheng, Philipp Klein, K. Plekhanov, K. Sengstock, M. Aidelsburger, C. Weitenberg and Karyn Le Hur, Phys. Rev. B 100, 08110 (R) (2019). Collaboration with Munich and Hamburg.

Bilayer system with M_1=M_2

$d_1 = d_2$

$M_1 = M_2$

$$\mathcal{H} = (\psi^\dagger_{\boldsymbol{k}1}, \psi^\dagger_{\boldsymbol{k}2})\mathcal{H}(\boldsymbol{k})\begin{pmatrix}\psi_{\boldsymbol{k}1}\\ \psi_{\boldsymbol{k}2}\end{pmatrix},$$

where $\psi^\dagger_{\boldsymbol{k}i} \equiv (c^\dagger_{\boldsymbol{k}Ai}, c^\dagger_{\boldsymbol{k}Bi})$ and

$$\mathcal{H}(\boldsymbol{k}) = \begin{pmatrix}(\boldsymbol{d}+M_1\hat{z})\cdot\boldsymbol{\sigma} & r\mathbb{I}\\ r\mathbb{I} & (\boldsymbol{d}+M_2\hat{z})\cdot\boldsymbol{\sigma}\end{pmatrix},$$

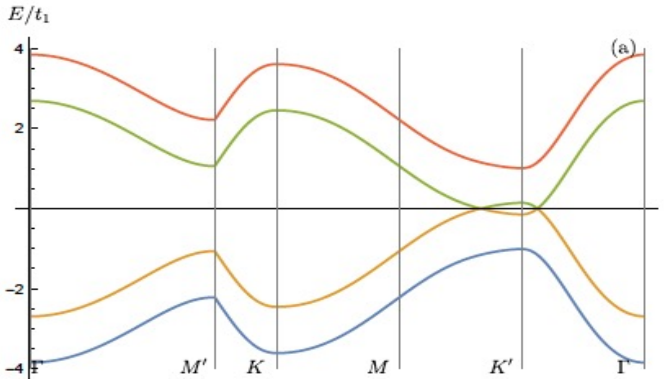

Joel Hutchinson & Karyn Le Hur
arXiv 2002.11823

Z_2

C=1/2

similar phase diagram

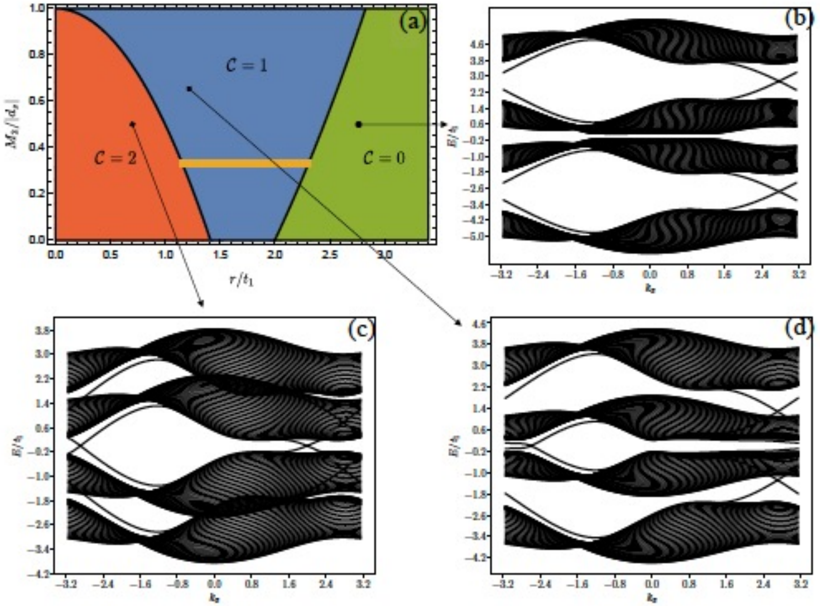

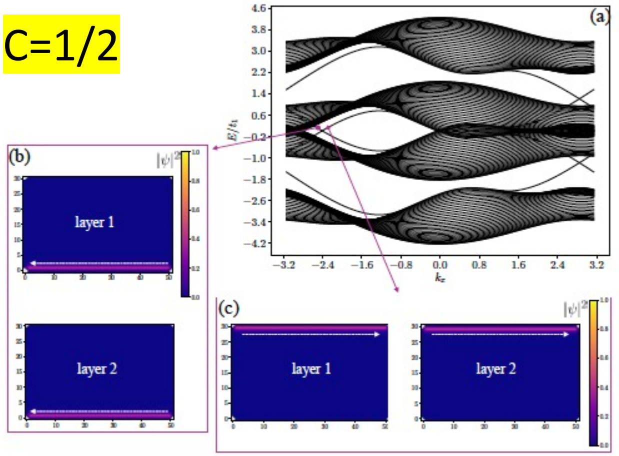

Also measurable with circular dichroism of light
Jones formalism

D. Tran, A. Grushin, P. Zoller & N. Goldman 2017
L. Asteria et al (Hamburg's group)
Ph. Klein, A. Grushin & K. Le Hur, 2021

Time-reversal invariant semimetals
S. Young and C. Kane, PRL 115, 126803 (2015)

Summary of geometry and Transport

$$j_{xy} = \frac{e}{2\pi} v^* \left(\mathcal{A}_\phi(0) - \mathcal{A}_\phi(\pi) \right) = \frac{(eC)}{2\pi} v^* = \frac{e^2}{h} CE$$

$C^j = \frac{1}{2}$

This formula is correct and is applicable in a given plane (sub-system j) from the poles (Dirac points)

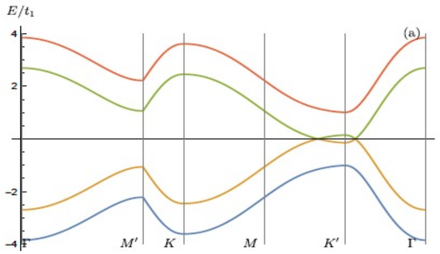

nodal ring region

$S \sim \ln 4$

$$\psi_1 = \frac{1}{\sqrt{2}}(0,-1,0,1), \quad \psi_2 = \frac{1}{\sqrt{2}}(0,1,0,1),$$
$$\psi_3 = \frac{1}{\sqrt{2}}(-1,0,1,0), \quad \psi_4 = \frac{1}{\sqrt{2}}(1,0,1,0).$$

$$|\psi_g\rangle = \tfrac{1}{2}(c^\dagger_{A1}c^\dagger_{B1} - c^\dagger_{A1}c^\dagger_{B2} - c^\dagger_{A2}c^\dagger_{B1} + c^\dagger_{A2}c^\dagger_{B2})|0\rangle$$

do not modify $n_B - n_A$

$$c^\dagger_{B1}c^\dagger_{B2}|0\rangle = |\uparrow\uparrow\rangle, \; c^\dagger_{A1}c^\dagger_{A2}|0\rangle = |\downarrow\downarrow\rangle, \; c^\dagger_{B1}c^\dagger_{A2}|0\rangle = |\uparrow\downarrow\rangle, \; c^\dagger_{A1}c^\dagger_{B2}|0\rangle = |\downarrow\uparrow\rangle.$$

$\frac{1}{\sqrt{2}}(\uparrow\downarrow + \downarrow\uparrow)$ K'

state at K

$$\tilde{C}^j = \frac{1}{2}\langle n^j_{KB} - n^j_{KA} - n^j_{K'B} + n^j_{K'A}\rangle = \frac{1}{2}$$

$r_c^- < r < r_c^+$

1/2 : plane

$j = 1/2$

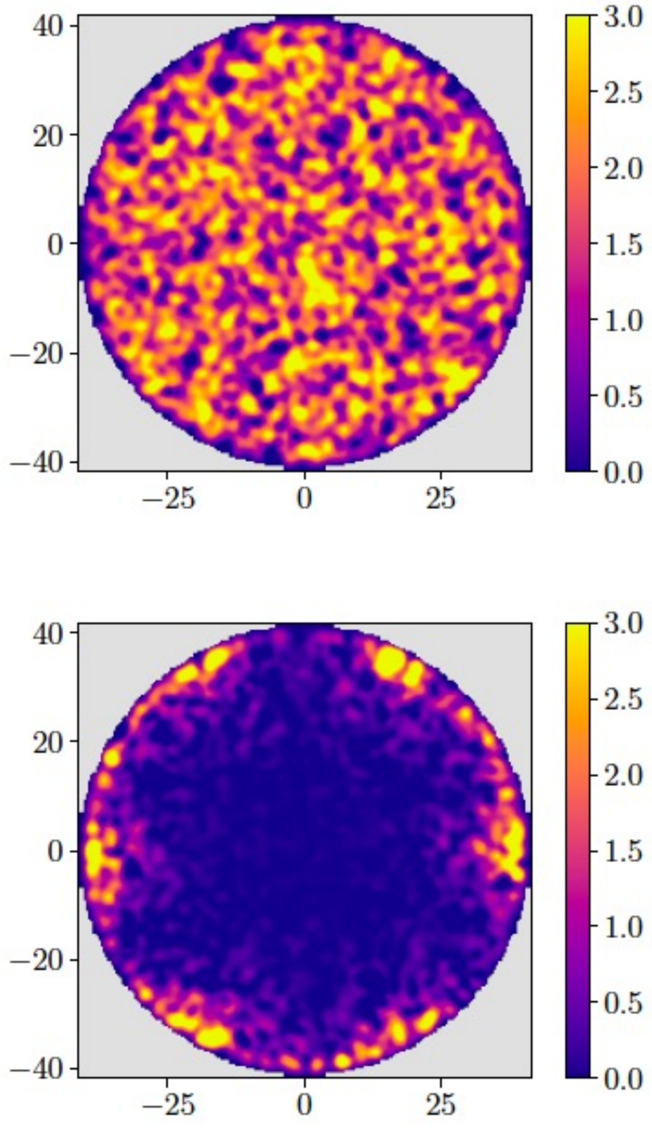

Figure 9: Top: Local density of states for a disk geometry with 30-site radius with $M_1 = M_2 = \sqrt{3}/3t_1$ and $r = 1.4t_1$ showing the edge mode and additional bulk states coming from the nodal ring semimetal in the reciprocal space. Bottom: Local density of states shifted very slightly from the line of symmetry: $M_2 = M_1 + 0.2$, $M_1 = \sqrt{3}/3t_1$ and $r = 1.4t_1$ in the blue region of the phase diagram, showing the single chiral edge mode.

Rational Numbers also occur for spin arrays

Resonating Valence Bond States

$$C^j = \frac{N+1}{2N},$$

$N = 5$

odd

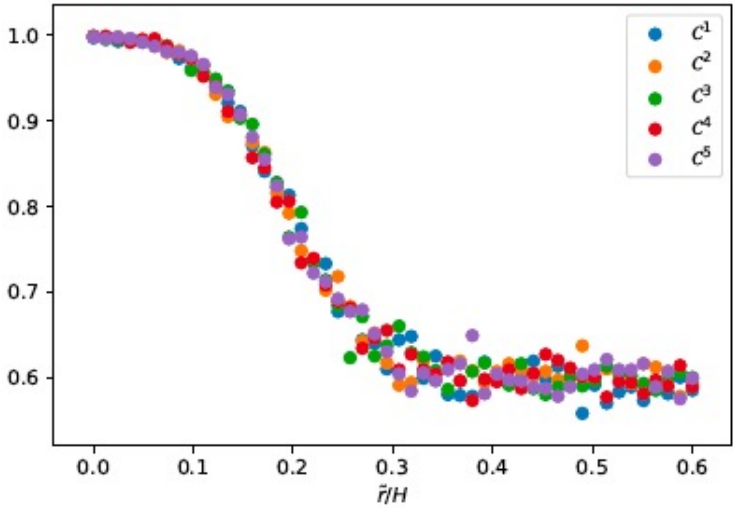

N even

$C^j = \frac{1}{2}$

Figure 12: Partial Chern numbers as a function of the coupling $\tilde{r}$ measured in a five-spins quantum circuit simulation with nearest-neighbour Ising interactions and periodic boundary conditions. To time-evolve the spins (qubits), we use a Trotter decomposition with 800 time steps and sweep velocity $v = 0.03H$. The bias field for all qubits is fixed to $M = 0.6H$. For $\tilde{r} \geq H - M \sim 0.4$ we verify the presence of the topological phase with $C^j = 3/5 = 0.6$ in agreement with Eq. (114).

Conclusion

Geometry of the sphere is also useful to understand topology of spin-1/2 models

- Application in quantum Transport

- Response to Circularly Polarized Light quantized

- Stochastic Approach to include Interaction Effects

Fractional Topology from the curved space, interactions between spheres
Applications: mesoscopic & atomic systems, topological semimetals

Thanks to the group members and new developments soon …

Thank You for your Attention